

Recent Solar Extreme Ultraviolet Irradiance Observations and Modeling: A Review

W. KENT TOBISKA

TELOS/Jet Propulsion Laboratory, Pasadena, California

For more than 90 years, solar extreme ultraviolet (EUV) irradiance modeling has progressed from empirical blackbody radiation formulations, through fudge factors, to typically measured irradiances and reference spectra as well as time-dependent empirical models representing continua and line emissions. A summary of recent EUV measurements by five rockets and three satellites during the 1980s is presented along with the major modeling efforts. The most significant reference spectra are reviewed and three independently derived empirical models are described. These include Hinteregger's 1981 SERF1, Nusinov's 1984 two-component, and Tobiska's 1990/1991 SERF2/EUV91 flux models. They each provide daily full-disk broad spectrum flux values from 2 to 105 nm at 1 AU. All the models depend to one degree or another on the long time series of the Atmosphere Explorer E (AE-E) EUV database. Each model uses ground- and/or space-based proxies to create emissions from solar atmospheric regions. Future challenges in EUV modeling are summarized including the basic requirements of models, the task of incorporating new observations and theory into the models, the task of comparing models with solar-terrestrial data sets, and long-term goals and modeling objectives. By the late 1990s, empirical models will potentially be improved through the use of proposed solar EUV irradiance measurements and images at selected wavelengths that will greatly enhance modeling and predictive capabilities.

INTRODUCTION

The requirement for an accurate estimate of the solar extreme ultraviolet (EUV) flux, a fundamental thermospheric energy input, is driven by the effort to provide a self-consistent model of the ionospheric and neutral atmospheric compositional and temperature structure that compares favorably with in situ and remotely sensed measurements. Research to understand the energy balance in the thermosphere has produced considerable activity over the past three decades to measure and model the solar EUV irradiance variations.

The broad spectrum of solar EUV irradiances at wavelengths below 105 nm has not been continuously measured since the Atmosphere Explorer E (AE-E) mission which ceased EUV observations in December 1980. The one exception has been the recent San Marco solar EUV experiment from March to December 1988. These measurements are just completing the calibration process. Short-duration rocket observations have been made on five occasions during the 1980s and these data sets serve as useful absolute reference points but do not contribute information about the long-term variations.

Given the paucity of continuously measured EUV data, a state of affairs termed the "EUV hole" by Donnelly [1987a] and graphically shown in Figure 1, three independently derived empirical solar EUV models have been developed which estimate the daily average full-disk flux variation for up to 39 wavelength groups or discrete lines at 1 AU. The model of Hinteregger *et al.* [1981] which was designated SERF1 by the World Ionosphere - Thermosphere Study (WITS) program called the Solar Electromagnetic Radiation Flux Study (SERFS), the Nusinov [1984] two-component model, and the EUV91 model [Tobiska, 1991], which evolved out of the SERFS program [Donnelly, 1988a] all utilize the AE-E EUV data set as either the only time-varying input to the

model (SERF1 and Nusinov) or as a significant component of the model (EUV91). All of the empirical solar EUV models are similarly limited to producing only full-disk emissions with daily average values often with a relatively coarse wavelength scale. The complexity in the models has increased with their attempt to reproduce solar rotational irradiance variations and other temporal phenomena. Additional complications have been introduced as the models attempt to reproduce emissions from specific solar temperature regions and from the evolution of disk features. Distinct periods in empirical solar EUV modeling are summarized by Simon and Tobiska [1991] including early theoretical description, data collection, and empirical modeling.

BACKGROUND

Early Theoretical Description (1900-1937)

The first empirically modeled, time-independent, solar EUV irradiance was described on October 19, 1900, at a meeting of the Berlin Physical Society. Planck, who had been searching for a way to reconcile the Wien and Rayleigh-Jeans formulations of the spectral distribution of blackbody radiation, revealed to the gathering an empirical formulation that fit quite well the experimental data of the day [Planck, 1901]. This function, Planck's law, is shown in Figure 2 compared with the Rayleigh-Jeans and Wien's energy densities and demonstrates the well-known equation

$$U(\lambda) = \frac{8\pi hc \lambda^{-5}}{e^{hc/\lambda kT} - 1} \quad (1)$$

This formulation, which assumed that the energy of an oscillator can only take on discrete values, set the stage for the quantum theory of light and solved the "ultraviolet catastrophe." This expressive term referred to the infinitely increasing UV energy with shorter wavelengths in the Rayleigh-Jeans formulation seen in Figure 2.

For several decades it was expected that the solar irradiance in the EUV followed the Planck blackbody spectrum. Finally, Saha [1937] noted that the only reasonable explanation for the forma-

Copyright 1993 by the American Geophysical Union.

Paper number 93JA01943.
0148-0227/93/93JA-01943\$05.00

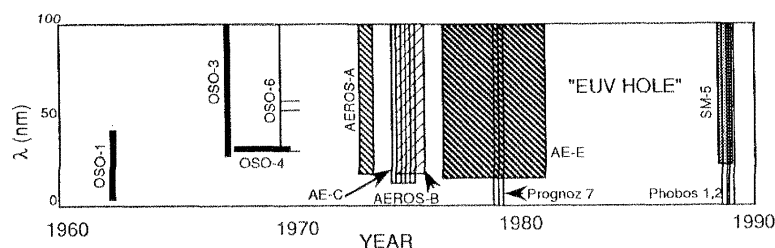


Fig. 1. Time and wavelength coverage of EUV measurements from satellites (adapted from *Schmidtke* [1992]).

tion of the first negative bands of nitrogen in the night sky observed at high-altitude sunrise and sunset ($z > 200$ km) was ionization from solar EUV ($0.1 < 66$ nm). His contribution to the field of empirical EUV modeling was based on estimating a photon flux value. He noted that the number of photons available for N_2 ionization, according to Planck's law, was insufficient given the total ion production rate needed to maintain a total ionization of 3×10^{10} electrons [*Chapman*, 1931]. Even if only 10% of the ionization were due to N_2 , Saha concluded that an "ultraviolet excess factor" of 1×10^6 more photons would be needed to maintain the ionization compared to the theoretical flux provided by a solar blackbody at 6500 K. Thus a "fudge factor" of a million times more photons in the EUV than those predicted by Planck's law became the next de facto EUV model.

Data Collection (1946-1980)

It was not until successful sounding rocket flights were made above the atmosphere that solar EUV observations were actually taken. The first solar UV flux from a sounding rocket was obtained shortly after the Second World War [*Baum et al.*, 1946]. These rocket experiments later led to the first EUV photographic spectra below 100 nm which were obtained through photographs sensitive in the FUV and later EUV. The early history is presented in a summary by *Tousey* [1961]. The first spectrophotometric solar EUV measurements down to 6 nm were presented by *Hinteregger* [1960] and the broad spectrum between 30 and 120 nm was described by *Hall et al.* [1963]. These observations were followed by rocket flights and satellite measurements that filled in spectral gaps or provided information leading to the revision of the earlier results. *Timothy* [1977] reviewed the history of observations from 30 to 120 nm through the mid-1970s.

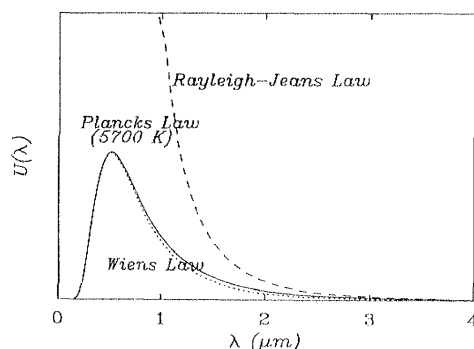


Fig. 2. Comparison of blackbody radiation for Planck's law, Wien's law, and Rayleigh-Jeans law. The Planck energy density spectrum fit experimental data of the day. Relative units of $U(\lambda)$ are in energy density. This spectral distribution is for a 5700 K blackbody (e.g., the Sun).

Figure 3 shows the solar spectrum published by *White* [1977] as a compilation of these early observations. The wealth of emission lines in the EUV, compared to the Planck solar blackbody in Figure 2, testifies to the remarkable observational progress in the three decades following World War II. Later, *Schmidtke* [1984], *Lean* [1987], *Rottman* [1988], and *Tobiska* [1991] summarized EUV observations from 10 to 120 nm through the mid-1980s. *Feng et al.* [1989] have provided a useful intercomparison of the integrated flux from 2 to 10 nm and 5 to 57.5 nm for many of the rocket observations of the 1970s and 1980s. *Schmidtke* [1992] has tabulated the observation periods, wavelength ranges, and results of the satellite missions monitoring the EUV during this same period.

Data Collection (1981-1989)

There are five rocket and three satellite data sets of the measured solar EUV irradiance that were obtained during the decade of the 1980s following the AE-E mission. In general, the rocket-measured irradiances have provided more accuracy in the measurements of the absolute solar flux below 57.5 nm and have provided calibration opportunities for one satellite data set which is just completing its calibration analysis.

The University of Southern California (USC) has flown three rocket experiments in 1982, 1983, and 1988. *Carlson et al.* [1984], *Ogawa and Judge* [1986], and *Ogawa et al.* [1990] describe these flights in detail. In brief, the August 10, 1982 flight occurred during high solar activity conditions where the 10.7-cm radio flux, $F_{10.7}$, was $210 \times 10^{22} \text{ W m}^{-2} \text{ Hz}^{-1}$. The instrument consisted of a windowless rare-gas (neon) ionization chamber to measure the total absolute EUV irradiance between 5 and 57.5 nm to $\pm 7\%$ uncertainty. The same instrument was reflown a year later on August 16, 1983, when the $F_{10.7}$ was 132 representing moderate to low solar activity conditions. The USC group flew a third rocket experiment on October 24, 1988, using a newly developed silicon photodiode to obtain the integrated absolute solar irradiance between 5 and 80 nm with an uncertainty of $\pm 14\%$. The $F_{10.7}$ of 168 on this date represented moderate solar activity.

The University of Colorado flew two rockets in 1988 [*Woods and Rottman*, 1990] and 1989 [*Woods and Rottman*, 1990; *T. N. Woods*, private communication, 1991] which measured solar EUV irradiance. The first, launched on November 10, 1988, included an EUV spectrograph that measured irradiances between 30 and 114 nm with an average wavelength-dependent uncertainty of $\pm 13\%$ and spectral resolution of 0.5 to 1 nm. The $F_{10.7}$ of 148 on this date represented moderate solar activity and this experiment has been used to calibrate the San Marco satellite EUV measurements discussed below. The second flight on June 20, 1989 used the same instrument when $F_{10.7}$ was 243 which represented high solar activity.

The San Marco 5 satellite carried the Airglow Solar Spectrometer Instrument (ASSI) during its mission between March and

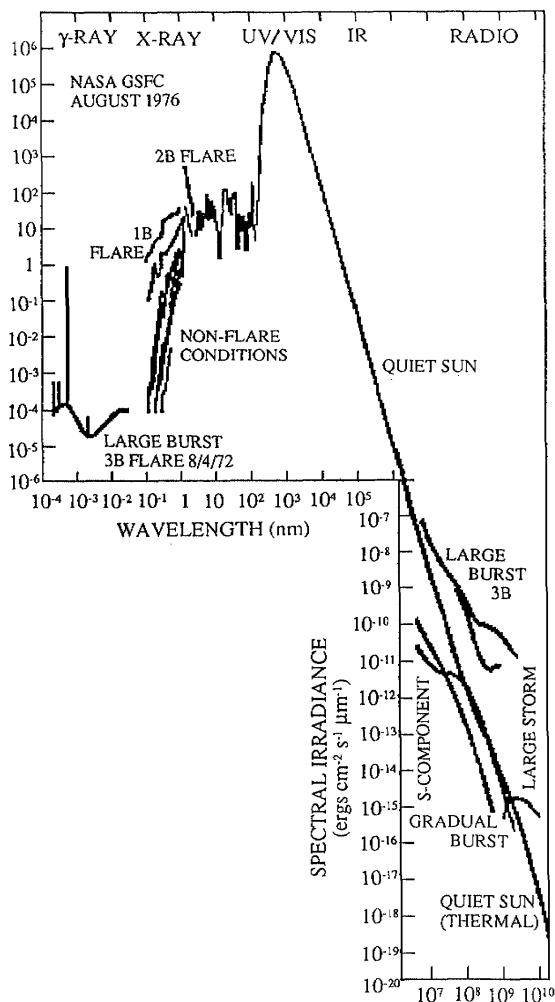


Fig. 3. The solar spectrum from gamma rays to radio wavelengths from White [1977].

December 1988. Schmidtke *et al.* [1985], Schmidtke *et al.* [1992], and Schmidtke *et al.* [1993] describe the instrument and preliminary results. The instrument consisted of two spectrometers covering the wavelength region of 28 nm to the visible with a resolution of approximately 1 nm. Preliminary conclusions (T. N. Woods, private communication, 1992) indicate that the contrast ratios for both chromospheric and coronal emissions measured by ASSI are similar to those derived using AE-E data, while daily deviations from simple empirical relationships are of the order of 30%.

The Prognos 7 satellite operated between November 1978 and February 1979 during high solar activity. It measured solar EUV irradiances with an instrument developed by the Institute of Applied Geophysics of the State Committee for Hydrometeorology using a thermoluminescent phosphorus $\text{CaSO}_4(\text{Mn})$ detector [Kazachevskaya *et al.*, 1985]. This instrument was sensitive to the integrated wavelength region of 1 to 130 nm; daily variability consistent with solar rotational effects has been described by Ivanov-Kholodny and Kazachevskaya [1981] and Kazachevskaya and Lomovsky [1992].

The Phobos 1 and 2 spacecraft en route to Mars (July to August 1988 and July 1988 to March 1989, respectively) carried the Solar

Ultraviolet Radiometer (SUFR) instruments that measured solar EUV irradiances on a daily basis and was particularly sensitive to solar flares at integrated wavelengths less than 130 nm. Kazachevskaya *et al.* [1991] and Kazachevskaya and Lomovsky [1992] describe the preliminary results of those observations during large M and X class flares.

MODELING

EUV Irradiance Modeling (Reference Spectra 1965-1992)

The first comprehensive review of solar EUV modeling was conducted by Schmidtke [1984] and covered the period through the early 1980s. A brief synopsis of the activities of this period is given here. Following a successful rocket observation of a broad EUV spectrum in 1963, Hinteregger *et al.* [1965] tabulated an EUV flux standard spectrum for quiet solar conditions. The early results were later revised and corrected, leading to a spectrum of "medium" solar activity with nonflaring conditions [Hinteregger, 1970]. This was followed by the Donnelly and Pope [1973] compilation of an EUV model spectrum for moderate solar activity that summarized numerous successful rocket and satellite observations up to the early 1970s. Figure 4 shows the Donnelly and Pope spectrum where moderate solar activity was defined when $F_{10.7}$ was 150. Hinteregger [1976] reviewed the advances in measuring EUV irradiances following the Atmospheric Explorer C (AE-C) mission in the mid-1970s while Heroux and Hinteregger [1978] released a revised reference spectrum for moderate solar activity based upon the detailed study of a 1974 rocket flight. Roble and Schmidtke [1979] contributed a description of a variety of typical EUV flux cases for different solar conditions applied to aeronautical calculations. The most recent reference spectrum [Schmidtke *et al.*, 1992] has been provided through the San Marco ASSI calibration based upon the Woods and Rottman [1990] sounding rocket data. Figure 5 shows this spectrum for moderate solar activity ($F_{10.7} \approx 150$) in 1-nm intervals.

Figure 5 shows that although there is general agreement in the overall magnitude of important emission features, there are also differences in the ASSI spectrum compared with SERF1. For example, the ASSI emission lines of Lyman- α (121.6 nm), Lyman- β

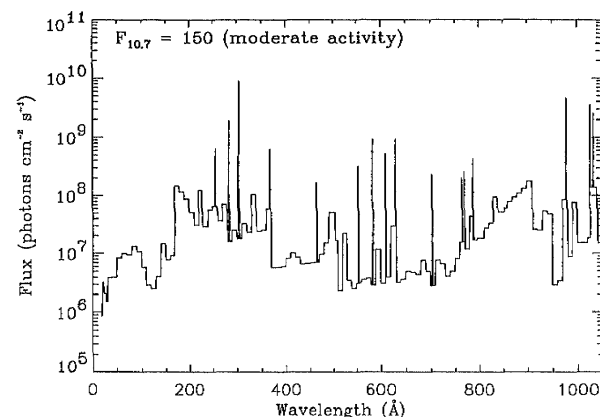


Fig. 4. Moderate solar activity spectrum compiled from several rocket observations [Donnelly and Pope, 1973]. Several discrete lines that are the most significant EUV emission lines in terms of magnitude are shown. The remaining flux (both lines and intervals) from Table 2 in Donnelly and Pope has been binned in 1-nm bins except for emissions below 3.1 nm where the average bin size is 0.3 nm. The abscissa wavelength conversion is $1 \text{ \AA} = 0.1 \text{ nm}$.

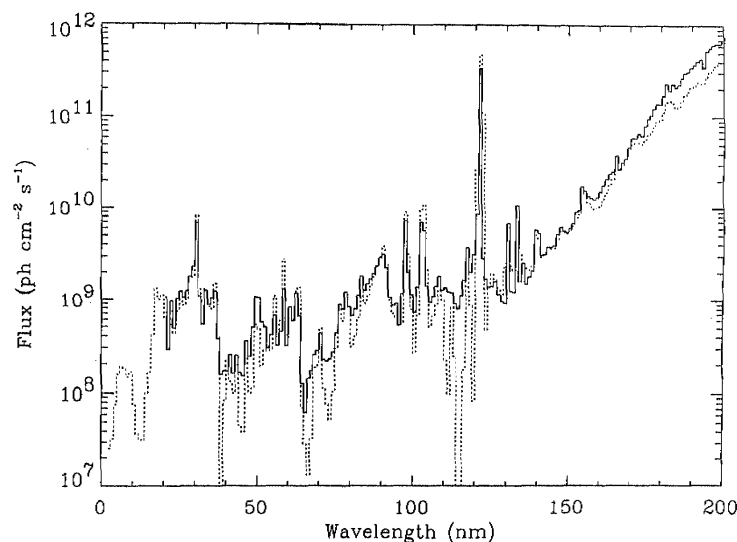


Fig. 5. ASSI solar EUV and FUV irradiance spectrum in 1 nm intervals (solid line) compared with modeled EUV flux from SERF1 (dashed line). The figure is from *Schmidtke et al.* [1992].

(102.6 nm), C III (97.7 nm), He I (58.4 nm), and He II (30.4 nm) all have smaller magnitude than SERF1. The He I and H Lyman continua have different slopes compared with each other. This suggests that the reference spectra and models still require a closer correspondence with one another.

As noted by *Simon and Tobiska* [1991], this period of EUV modeling was characterized by the presentation of reference spectra under a variety of solar conditions, by the categorizing of quiet, moderate, and active solar condition spectra, and by the description of the primary line and continua emission features. Important morphological features of the irradiance time series from satellite observations were described by *Timothy* [1977] including the 27-day variation corresponding to solar rotational effects with a peak-to-valley ratio of $\pm 15\%$ for emissions originating in the solar chromosphere and the hint of active region evolution on longer time scales. *Rottman* [1988] noted that the EUV irradiances varied with the 11-year solar cycle and had a maximum-to-minimum ratio ranging from a factor of 2 to greater than 10 depending upon the solar source region for the wavelength.

By the end of the 1970s, it had become customary to represent solar EUV flux with the $F_{10.7}$ values [*Neupert*, 1967; *Hall and Hinteregger*, 1970; *Chapman and Neupert*, 1974; *Schmidtke*, 1976], although it has been pointed out [*Timothy*, 1977; *Donnelly*, 1982; *Donnelly et al.*, 1986a] that the $F_{10.7}$ is an unreliable indicator of EUV irradiance variability. *Hedin* [1984], *Donnelly et al.* [1986b], *Donnelly* [1987b], *Tobiska* [1988, 1990], *Tobiska and Barth* [1990], and *Donnelly and Puga* [1990] additionally describe the correlations of full-disk EUV irradiances with $F_{10.7}$. *Neupert* [1992] describes in detail the correlations between specific solar EUV emission lines and the solar 10.7- and 21-cm measurements in one spatial dimension.

Despite the tremendous observational advances of the period, the primary weaknesses that existed in solar EUV modeling could be attributed to the lack of long-term daily irradiance measurements combined with limited proxy representation of the flux. Reference spectra represented general levels of solar activity and provided more spectral detail than had been previously available.

EUV Irradiance Proxies

Prior to a continued discussion of EUV irradiance modeling, and particularly related to the effort to improve proxy representation of EUV flux, it is useful to describe those proxies, or indices, which have been correlated to various EUV emissions. Just as modeling has evolved over time, so has the use of proxies in order to estimate the EUV irradiances.

The most common proxy of solar EUV irradiance is the $F_{10.7}$ which was previously called the Covington index. The 27-day variability in this solar radiometric emission, coincident with the appearance of sunspots, was first described from ground-based daily measurement during the late 1940s [*Covington*, 1948]. The daily $F_{10.7}$, formerly measured regularly at the Algonquin Observatory in Ottawa since February 1947, is now measured with automated equipment at the Penticton (British Columbia) observatory since June 1991. *Gelfreikh* [1992] reviews the observational methods of solar radio astronomy and includes the main mechanisms for radio radiation generation. *Tapping* [1987] describes the two primary emission components of bright, compact sources and weaker, diffuse emission of the $F_{10.7}$.

The early connections of $F_{10.7}$ with the EUV irradiances were made through a sequence of events. *Roemer et al.* [1983] summarize some of the early connections between the solar EUV, the decimetric indices, and the thermospheric density variations. First, observations of 27-day variations in satellite drag [*Jacchia*, 1958] were linked to solar rotational radiation variation in $F_{10.7}$. This 1958 article referred to a previous suggestion that the thermospheric densities actually varied, although it was known at the time that $F_{10.7}$ did not contribute to heating, ionization, nor dissociation processes in the atmosphere. Much more energetic radiation in the UV and EUV was needed to accomplish those tasks. The first conclusive evidence of solar EUV irradiance (He I 30.4 nm, Fe XV 28.4 nm, and Fe XVI 33.5 nm) variation with a 27-day periodicity corresponding to the $F_{10.7}$ and sunspot solar rotational variability was obtained by the OSO 1 satellite [*Neupert et al.*, 1964].

By the late 1970s, modelers [Hinteregger *et al.*, 1981; (H. E. Hinteregger, private communication for the World Ionosphere-Thermosphere Study (WITS) Solar Electromagnetic Radiation Flux Study (SERFS) program, 1985)] began using other proxies for EUV variability including several that came from space-based observations. The AE-E-measured Lyman- β (102.6 nm) and the Fe XVI (33.5 nm) emissions were selected by Hinteregger to represent similar solar temperature regions, i.e., the chromospheric and the coronal emissions, respectively. Later, Tobiska [1988] explored the use of satellite-measured Lyman- α (121.6 nm) and 0.1 to 0.8 nm X rays to represent chromospheric and coronal EUV emissions since the proxy emissions selected by Hinteregger were no longer available on a regular basis.

H I Lyman- α (121.6 nm), H I Lyman- β (102.6 nm), Fe XVI (33.5 nm), and 0.1 to 0.8 nm X ray emissions must all be measured above the atmosphere by satellites. There is an exhaustive literature set covered by several reviews describing the production mechanisms [e.g., Vernazza *et al.*, 1981; Fontenla *et al.*, 1990, 1991], the observations, and the variability of the Lyman- α emission [e.g., Vidal-Madjar, 1977; Lean and Skumanich, 1983; Lean, 1987; Rottman, 1987; Barth *et al.*, 1990]. The 0.1 to 0.8 nm X ray measurements are also described in an extensive literature base [e.g., Kreplin *et al.*, 1977; Donnelly, 1981; Donnelly and Bower, 1981; Wagner, 1988; Kreplin and Horan, 1992; Kahler, 1992].

An important ground-based proxy which has been correlated with chromospheric emissions is the equivalent width (EW) of the He I 1083-nm line, the measurements of which are described by Harvey [1984] and the formation in the solar atmosphere of which is described by Vernazza *et al.* [1981] and by E.H. Avrett (private communication, 1993). Other ground-based measurements of chromospheric EUV proxies include the Ca II K 0.1-nm index as described or summarized by White and Livingstone [1978, 1981], Keil and Worden [1984], and White [1987] and the solar plage index based on the Ca II K line [e.g., White, 1987]. Space-based measurements of the Mg II core-to-wing ratio (*c/w*) at 280 nm have also provided a reliable proxy for solar EUV chromospheric irradiances [e.g., Heath and Schlesinger, 1986; Donnelly, 1988b]. Ground-based measurements of the 530.3-nm green line coronal index (CI) summarized by Rusin and Rybansky [1992] and Rybansky and Rusin [1992] are a potential coronal proxy currently being considered (R. F. Donnelly, private communication, 1991). Finally, the correlations between solar UV and EUV emissions and several of the ground- and space-based proxies have been extensively discussed or reviewed by Donnelly *et al.* [1983, 1985], Donnelly [1987b], White [1987], Tobiska [1988, 1990], and Lean [1987], for example.

EUV Irradiance Modeling (Proxy Correlation 1979-1992)

The first complete empirical solar EUV model was developed by Hinteregger *et al.* [1981] and fully documented by H. E. Hinteregger (private communication for the World Ionosphere-Thermosphere Study (WITS) Solar Electromagnetic Radiation Flux Study (SERFS) program, 1985) following the completion of the AE-E mission. A substantial contribution of this work was the publication of the cycle 21 solar minimum reference spectrum SC#21REFW as shown in Figure 6. The emission lines from highly ionized elements and the continua features in Figure 6 are a result of magnetic activity originating below the surface, coupling with the solar atmosphere, and exchanging that energy in complex processes. Linsky [1977], Spruit [1987], and Zirin [1987] outline general, theoretical reviews of the processes producing these EUV lines and continua. The detailed identification of these emission

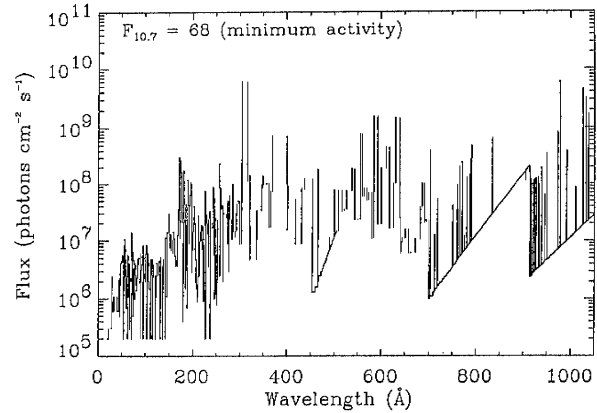


Fig. 6. This spectrum represents the July 1976 period from SERF1 with a 0.1-nm wavelength grid where several wavelengths are missing. The total integrated flux from 5 to 57.5 nm for this spectrum is $15.0 \times 10^9 \text{ ph cm}^{-2} \text{ s}^{-1}$.

lines and continua can be found by Kelly [1968], Hinteregger [1969], and Kurucz [1991].

Emerging from Hinteregger's work was an EUV "class" model combined with a two-variable $F_{10.7}$ "association" formula for estimating the EUV flux. The EUV class model was limited to the time frame of the AE-E mission between July 1977 through December 1980. The irradiance values of the EUV class relationship are described in photons $\text{cm}^{-2} \text{ s}^{-1}$ by

$$I_{\lambda} = I_{\lambda \text{ref}} + I_{\lambda \text{ref}} (R_k - 1) C(\lambda) \quad (2)$$

where $I_{\lambda \text{ref}}$ is the EUV flux at solar cycle minimum. R_k is the ratio for a specific date of a key EUV flux to the solar minimum value. $C(\lambda)$ is a wavelength-dependent scaling parameter for each EUV wavelength. The two key, k , emissions are H Lyman- β and Fe XVI where the Lyman- β flux was used to estimate other chromospheric emission intensities, and the Fe XVI (33.5 nm) line was used to estimate other coronal and transition region (hereafter referred to as coronal) emission intensities.

The association formula (H. E. Hinteregger, private communication for the World Ionosphere-Thermosphere Study (WITS) Solar Electromagnetic Radiation Flux Study (SERFS) program, 1985) used both $F_{10.7}$ daily and 81-day mean values in a linear correlation with AE-E EUV flux values in order to estimate EUV irradiances outside the AE-E time frame. This irradiance association formulation is described by

$$I_{\lambda} = A_{\lambda} F_{10.7}^* + B_{\lambda} (F_{10.7} - F_{10.7}^*) + C_{\lambda} \quad (3)$$

where $F_{10.7}$ is the daily value and $F_{10.7}^*$ is its 81-day mean value. A_{λ} , B_{λ} , and C_{λ} are obtained from a least squares fit to the AE-E EUV data. This model was reviewed by Schmidtke [1984] and more recently summarized by Rottman [1988] and Tobiska and Barth [1990]. In the late 1980s, Hinteregger's model was designated the SERF1 EUV model [Donnelly, 1988a].

Following the release of Hinteregger's AE-E data, Nusinov [1984] developed a two-component model of full-disk solar EUV irradiance variation based upon nonlinear regression formulas between $F_{10.7}$ and the AE-E EUV data set. In this second independently derived model, he developed radio background and active region components such that the EUV wavelengths for seven dis-

crete lines could be modeled with time variation. An empirically determined function that fit the $F_{10.7}$ background provided a new capability for predicting this background component. Figure 7 shows the Nusinov $F_{10.7}$ background component (chromospheric network), and (4) describes his irradiance model as

$$I_{\lambda} = B_0 + B_1 (F_b - A)^{2/3} + B_2 (F_{10.7} - F_b)^{2/3} \quad (4)$$

where the first term is the background component, the second term is the active region component, and the A , B_0 , B_1 , and B_2 coefficients are found in the work by Nusinov [1984].

The Nusinov background component is

$$F_b = 63 + 482 \sin^{3.7}(\pi t/T) e^{-5.2t/T} \quad (5)$$

where t is time in years from the beginning of the cycle and T is the period of the cycle also in years. Bruevich and Nusinov [1984] extended this model throughout the EUV from 10 to 105 nm and Nusinov [1992] extended the model between 1 and 10 nm in addition to providing a method for determining the F_b background component for cycles 20 and 21.

The third independent modeling effort by Tobiska [1988] was characterized by the development of a two-index EUV flux model based on the Hinteregger *et al.* [1981] class model concept and the AE-E data set. It used the H Lyman- α to estimate the chromospheric irradiances and 0.1 to 0.8 nm X rays to estimate the coronal irradiances. Tobiska and Barth [1990] changed and improved this model by replacing the 0.1 to 0.8 nm X ray index with the $F_{10.7}$ daily values for use in estimating coronal EUV fluxes and by incorporating additional rocket EUV measurements to lower the uncertainty of the absolute irradiance values. This fourth empirical model by Tobiska and Barth was subsequently designated SERF2 [R.F. Donnelly, private communication, 1989; Tobiska and Barth, 1990] and covered the time frame between October 1981 and April 1989. Tobiska [1990] detailed the SERF2 model development.

SERF1 and SERF2 were compared by Lean [1990] over timescales of the 27-day solar rotation and the 11-year solar cycle. Significant differences were found between the models and between each model and the data sets upon which they were based. The differences appeared in the estimation of absolute intensities, the magnitude of peak-to-valley variation of irradiance due to solar rotation, and the maximum-to-minimum flux values over the 11-year solar cycle. Lean concluded that neither the models nor measurements yet provided a consistent picture of long-term variability in the EUV portion of the Sun's spectrum.

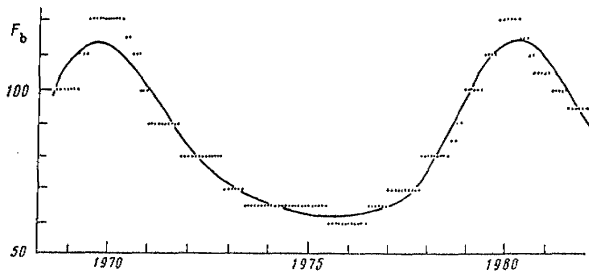


Fig. 7. Nusinov [1984] provided a $F_{10.7}$ background emission which is representative of the chromospheric network. He determined an empirical fit to the data given in (5) in the text. The units of F_b are $1 \times 10^{-22} \text{ W m}^{-2} \text{ Hz}^{-1}$. The abscissa value is time labeled with years.

In an effort to address the weaknesses of SERF2 and in order to assist the evaluation of the solar data from the San Marco Airglow Solar Spectrometer Instrument (ASSI) [Tobiska *et al.*, 1993], the SERF2 model was substantially revised [Tobiska, 1991]. This fifth model, called EUV91, represents an advance over the previous EUV models in proxy use, modeling technique, consistency of model results with data sets, and ability to incorporate into the model new solar data sets and recent proxy measurements. The model extends from 1947 to the present for coronal EUV full-disk irradiances and from 1976 to the present for chromospheric EUV full-disk irradiances. The solar Lyman- α (121.6 nm) emission line and He I 1083-nm EW measurements are used as the independent model parameters for the chromospheric irradiances while the $F_{10.7}$ daily and 81-day running mean values are the independent parameters for the coronal and transition region irradiances. The results of the model are full-disk photon fluxes at 1 AU for 39 EUV wavelength groups and discrete lines between 1.8 and 105 nm for a given date. Data from the OSO1/3/4/6, AEROS A, AE-E satellites and six rocket data sets are used in the model development. The irradiances from this model are given as

$$F(\lambda, t) = a_0(\lambda) + \sum_{i=1}^4 a_i(\lambda) F_i(t) \quad (6)$$

where $F_i(t)$ are the proxy data sets. For example, $F_1(t)$ is Lyman- α , $F_2(t)$ is He I 1083-nm EW scaled to Lyman- α values, $F_3(t)$ is daily $F_{10.7}$, and $F_4(t)$ is the 81-day running mean value of $F_{10.7}$. The $a_i(\lambda)$ coefficients are tabulated by Tobiska [1991]. Missing proxy data are substituted through an empirical relationship with another proxy for which data exist on given dates. Figure 8 shows three examples of this model under low, moderate, and high solar activity conditions on the same wavelength scale as SC#21REFW. As a detailed example, Table 1 lists the EUV91 irradiance values for the moderate solar activity case on November 10, 1988, i.e., the date of the LASP rocket [Woods and Rottman, 1990]. Figure 9, adapted from Ogawa *et al.* [1990], shows a comparison of the model with several rocket flights and two previous models, i.e., those of Donnelly and Pope [1973] and SC#21REFW [Hinteregger *et al.*, 1981], for the 5 to 57.5 nm integrated flux.

A sixth model, SERF3, is presently under development as a full-disk multiple proxy model for chromospheric and coronal emissions. It correlates Mg II (c/w), Ca K 0.1 nm index, He I 1083-nm EW, $F_{10.7}$, 530.3-nm, and 0.1- to 0.8-nm data with the AE-E data set (R. F. Donnelly, private communication, 1993).

The SERF program concluded with the end of WITS on December 31, 1989. Since then, much of the international collaborative effort to study long-term changes in the solar total and spectral irradiance has been centered in the Solar Electromagnetic Radiation Study 22 (SOLERS22). The SOLERS22 program, a project of the Solar-Terrestrial Energy Program (STEP), has posed two questions to define its work: What are the daily flux values of the solar spectral irradiance in the X ray, EUV, UV, visible and infrared wavelength ranges and the total solar irradiance? and What evolving solar spatial structures cause the temporal variations of these full-disk fluxes? One project objective is to develop improved solar flux models for the irradiance variations.

In general, this period of proxy correlation concluded with important advances. A common strength of all six models is that each uses multiple indices to estimate solar EUV emissions whose source regions are in different temperature layers of the solar atmosphere. Each model represents, to first order, the 27-day (solar rotation), intermediate-term (active region evolution and decay), and long-term 11-year (solar cycle) relative variability of the ir-

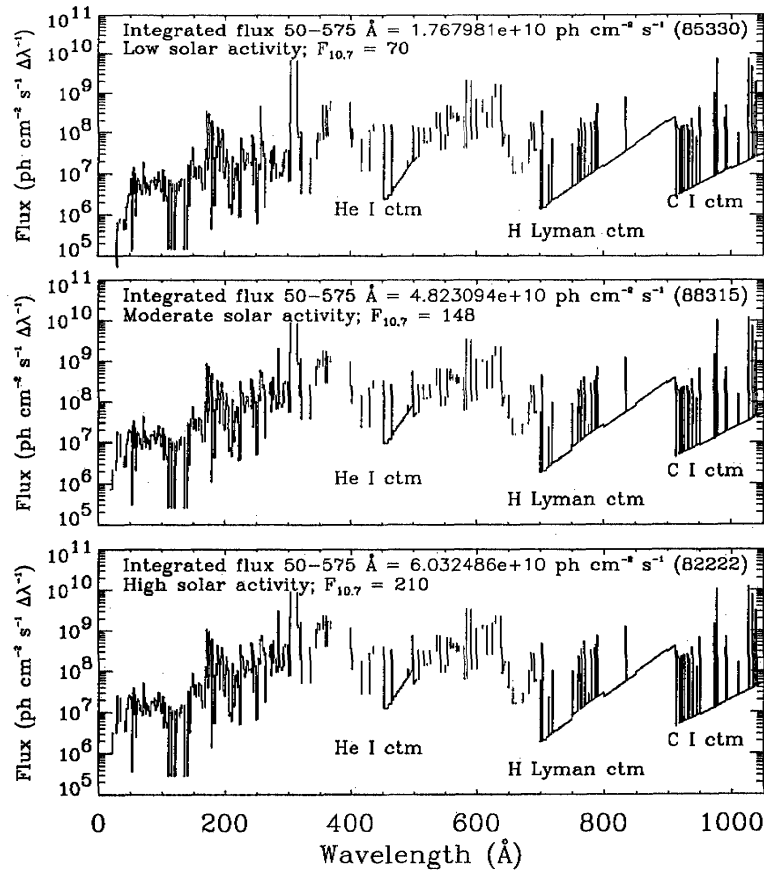


Fig. 8. The EUV91 model solar EUV spectrum for November 26, 1985 (low solar activity), for November 10, 1988 (moderate activity), and for August 10, 1982 (high activity) are shown in three panels. The total integrated flux for 5 to 57.5 nm is 17.7×10^9 ph cm⁻² s⁻¹ for the November 1985 case, 48.2×10^9 ph cm⁻² s⁻¹ for the November 1988 case, and 60.3×10^9 ph cm⁻² s⁻¹ for the August 1982 case. The He I continuum is visible between 45 and 50.4 nm, the H Lyman continuum is between 70 and 91.2 nm, and the C I continuum is between 91.3 and 105 nm in each panel. Discrete emission lines rise considerably higher than the continua. The modeled spectrum is based on the wavelength ranges of the SC#21REFW spectrum and contains missing lines.

radiance. Each model also estimates the magnitude, phase, rise, and decline of the measured EUV emissions with uncertainty (compared to the data and neglecting the uncertainty of the data) from less than $\pm 10\%$ to greater than a factor of ± 2 depending upon wavelength and model. Several generally reliable ground- and space-based proxies have been found for the chromospheric and coronal emissions that are now in use or are being developed for use in models. Lyman- α and He I 1083-nm EW emissions were found to be good full-disk indices for chromospheric emissions and $F_{10.7}$ daily and 81-day mean values were found to be acceptable indices for transition region and coronal emissions.

Current EUV models are specifically designed for use by the aeronomy community to provide thermospheric energy inputs. The solar models provide irradiances at a variety of spectral resolutions for campaign dates, solar maximum to minimum periods, and terrestrial seasonal time frames. On the basis of the models and data available at the end of the 1980s, *Lean* [1988] and *Tobiska* [1988] graphically show spectral irradiance ratios for solar maximum to minimum by wavelength and show unit optical depth penetration into the terrestrial atmosphere for the EUV wavelengths during solar maximum and minimum conditions.

There are a number of weaknesses still remaining in the models. First, each of the models has inconsistencies, often in absolute magnitude of emission, between modeled flux values and observed data. In large part, these inconsistencies can be traced to phase and amplitude differences in temporal variation between proxies and data; they can also be traced to errors of approximation which are inherent in linear or nonlinear regression techniques as applied to the proxy-data correlations. Additionally, sparse or discontinuous EUV data also contribute to model uncertainty. These missing data combine with flux magnitude disagreements between the independent EUV data sets that are used in model correlations. Weighting some data sets over others further magnifies modeling uncertainties.

A second weakness is that two of the models (SERF1 and Nusinov) rely solely on one data set (AE-E) for temporal variation and for all flux absolute magnitudes. The other models are heavily influenced by the AE-E data set for temporal variation and rely on one rocket measurement for absolute magnitudes below 15 nm at any spectral resolution.

A third weakness is that limited comparison between the solar EUV models and their inputs into thermospheric/ionospheric

TABLE 1. EUV91 Modeled Irradiances for November 10, 1988

λ^*	Φ^\dagger	λ	Φ	λ	Φ	λ	Φ	λ	Φ
18.62	7.22E+05	67.14	9.22E+06	90.14	9.53E+06	127.65	1.18E+07	193.52	1.84E+08
18.97	7.22E+05	67.35	6.15E+06	90.45	6.15E+06	129.87	8.88E+06	195.13	3.01E+08
21.6	2.16E+06	68.35	7.07E+06	90.71	9.22E+06	130.3	2.61E+05	196.52	2.73E+07
21.8	7.22E+05	69.65	4.24E+07	91	1.20E+07	131.02	1.36E+07	196.65	8.17E+06
22.1	2.16E+06	70	3.07E+05	91.48	5.84E+06	131.21	1.25E+07	197.44	1.13E+07
28.47	3.61E+06	70.54	1.01E+07	91.69	1.66E+07	136.21	2.61E+05	198.58	2.00E+07
28.79	1.80E+07	70.75	9.22E+06	91.81	1.48E+07	136.28	2.61E+05	200.02	6.32E+07
29.52	1.59E+07	71	1.35E+07	92.09	1.17E+07	136.34	2.61E+05	201.13	1.07E+08
30.02	3.88E+06	71.94	3.69E+06	92.81	1.17E+07	136.45	2.61E+05	202.05	1.66E+08
30.43	2.59E+06	72.31	1.97E+07	93.61	1.72E+07	136.48	2.61E+05	202.64	9.31E+07
33.74	4.74E+06	72.63	4.92E+06	94.07	2.52E+07	141.2	2.95E+07	203.81	8.22E+07
40.95	2.59E+06	72.8	6.46E+06	94.25	3.07E+05	144.27	2.87E+06	204.25	3.03E+07
43.76	9.06E+06	72.95	1.05E+07	94.39	5.23E+06	145.04	3.68E+07	204.94	2.06E+07
44.02	3.45E+06	73.47	1.54E+06	94.9	3.07E+05	148.4	7.68E+07	206.26	6.32E+06
44.16	3.88E+06	73.55	5.84E+06	95.37	1.48E+07	150.1	2.14E+07	206.38	6.32E+06
45.66	2.16E+06	74.21	7.69E+06	95.51	8.92E+06	152.15	3.69E+07	207.46	6.32E+06
46.4	1.16E+07	74.44	4.00E+06	95.81	8.92E+06	154.18	1.94E+07	208.33	7.58E+06
46.67	1.73E+07	74.83	1.23E+07	96.05	2.52E+07	157.73	1.75E+07	209.63	3.79E+06
47.87	1.94E+07	75.03	1.41E+07	96.49	5.84E+06	158.37	4.00E+07	209.78	4.63E+06
49.22	1.85E+07	75.29	7.69E+06	96.83	8.30E+06	159.98	3.66E+07	211.32	1.15E+08
50.52	1.72E+07	75.46	1.17E+07	97.12	1.60E+07	160.37	3.10E+07	212.14	3.37E+07
50.69	1.72E+07	75.73	7.69E+06	97.51	9.22E+06	162	1.55E+07	213.78	1.05E+07
52.3	1.08E+07	76.01	9.84E+06	97.87	7.07E+06	164.15	1.04E+07	214.75	1.81E+07
52.91	3.07E+05	76.48	3.07E+06	98.12	8.30E+06	167.5	5.49E+07	215.16	6.11E+07
54.15	2.52E+07	76.83	1.26E+07	98.26	8.30E+06	168.17	1.01E+08	216.88	4.21E+07
54.42	1.11E+07	76.94	1.01E+07	98.5	7.99E+06	168.55	5.77E+07	218.19	7.79E+07
55.06	1.23E+07	77.3	8.92E+06	99.71	6.15E+06	168.92	3.55E+07	219.13	3.03E+07
55.34	3.26E+07	77.74	1.20E+07	99.99	8.30E+06	169.7	6.59E+07	220.08	4.34E+07
56.08	7.38E+06	78.56	9.22E+06	100.54	2.19E+07	171.08	8.66E+08	221.44	7.50E+07
56.92	2.28E+07	78.7	8.61E+06	103.01	3.92E+06	172.17	3.15E+07	221.82	3.79E+06
57.36	1.91E+07	79.08	5.84E+06	103.15	2.61E+05	173.08	6.03E+07	224.74	1.76E+08
57.56	1.54E+07	79.48	5.53E+06	103.58	1.59E+07	174.58	7.57E+08	225.12	3.22E+08
57.88	1.32E+07	79.76	7.07E+06	103.94	1.59E+07	175.26	9.32E+07	227.01	1.75E+08
58.96	2.15E+06	80	4.30E+06	105.23	1.33E+07	177.24	4.58E+08	227.19	8.43E+05
59.62	2.15E+06	80.55	7.07E+06	106.25	5.22E+06	178.05	5.77E+07	227.47	1.24E+08
60.3	7.69E+06	82.43	1.51E+07	108.05	3.92E+06	179.27	1.13E+06	228.7	8.59E+07
60.85	1.11E+07	82.74	7.99E+06	109.98	2.61E+05	179.75	5.80E+07	230.65	5.48E+07
61.07	1.78E+07	82.84	7.99E+06	110.56	2.61E+05	180.41	5.04E+08	231.55	6.66E+07
61.63	8.92E+06	83.42	1.38E+07	110.62	2.61E+05	181.14	5.97E+07	232.6	9.69E+07
61.9	1.54E+07	83.67	1.17E+07	110.76	3.92E+06	182.17	6.51E+07	233.84	1.52E+07
62.3	3.07E+05	84	1.57E+07	111.16	2.61E+05	183.45	4.22E+06	234.38	1.39E+08
62.35	3.38E+06	86.77	1.41E+07	111.25	1.25E+07	184.53	1.23E+08	237.12	1.64E+07
62.77	1.05E+07	86.86	5.84E+06	113.8	7.84E+06	184.8	6.48E+06	237.2	8.43E+05
63.16	1.01E+07	86.98	9.53E+06	114.09	6.79E+06	185.21	5.13E+07	237.33	8.13E+07
63.3	1.66E+07	87.3	7.38E+06	114.24	2.61E+05	186.6	9.01E+06	239.87	8.43E+07
63.65	1.26E+07	87.61	6.15E+06	115.39	2.61E+05	186.87	6.51E+07	240.71	7.04E+07
64.11	3.38E+06	88.09	1.38E+07	115.82	6.27E+06	187.95	1.97E+06	241.74	3.77E+08
64.6	7.69E+06	88.11	1.88E+07	116.75	1.02E+07	188.23	2.73E+07	243.03	3.67E+08
65.21	9.22E+06	88.14	3.07E+05	117.2	6.79E+06	188.31	3.38E+08	243.78	2.40E+07
65.71	1.26E+07	88.42	5.84E+06	120.4	2.61E+05	190.02	1.19E+08	244.92	2.44E+08
65.85	9.22E+06	88.64	7.38E+06	121.15	2.61E+05	191.04	2.96E+07	245.94	4.21E+06
66.26	9.22E+05	88.9	1.17E+07	121.79	2.87E+06	191.34	2.53E+07	246.21	9.61E+07
66.3	1.17E+07	89.14	8.30E+06	122.7	1.07E+07	192.4	1.13E+08	246.91	4.93E+07
66.37	1.23E+06	89.7	9.22E+06	123.5	6.79E+06	192.82	1.66E+08	247.18	1.05E+08

models has been done. This is in spite of the fact that there is widespread aeronomy community use of the solar minimum and solar maximum reference spectra that were derived from the AE-E data set [e.g., Roble, 1987; Donnelly, 1987a]. Donnelly (private communication, 1990) noted that SERF1 and SERF2 concentrated on relative temporal variations rather than absolute fluxes and that no comparisons with spatially resolved solar measurements had yet been made. In addition, no terrestrial atmosphere model evaluations using these temporal solar flux models had been completed by the end of the decade.

Buonsanto *et al.* [1992] have begun this process of comparing atmospheric data sets and solar EUV models and have obtained interesting results. They compared measured and modeled electron densities in the $E-F_1$ region ionosphere. The modeled electron densities were produced by two separate photochemical models using SERF1, EUV91, and rocket-measured solar EUV flux. They concluded that although the photochemical models generally underestimated the atmospheric data, especially in winter, the model results were an improvement over previous work when the new solar data were used. In particular, since the EUV91 model pro-

TABLE 1. (continued)

λ^*	Φ^\dagger	λ	Φ	λ	Φ	λ	Φ	λ	Φ
249.18	5.06E+06	401.14	9.33E+07	499	8.55E+07	712.7	2.29E+07	761	1.04E+07
251.1	5.13E+06	401.94	2.47E+08	499.37	5.76E+08	713	2.58E+06	761.13	5.11E+07
251.95	1.46E+08	403.26	1.44E+08	500	4.24E+07	714	2.58E+06	762	1.06E+07
252.19	1.03E+08	417.24	2.38E+07	501	4.49E+07	715	2.77E+06	762.01	7.69E+07
253.78	1.06E+08	430.47	2.22E+08	502	4.70E+07	716	2.77E+06	763	1.08E+07
256.32	5.92E+08	436.7	3.31E+08	503	4.95E+07	717	2.77E+06	764	1.12E+07
256.38	2.33E+08	453	9.67E+06	504	5.27E+07	718	3.14E+06	765	1.15E+07
256.64	9.61E+07	454	9.67E+06	507.93	2.71E+08	718.5	9.80E+07	765.15	3.28E+08
256.92	1.60E+07	455	9.67E+06	515.6	1.18E+08	719	3.14E+06	766	1.17E+07
257.16	4.21E+08	456	9.67E+06	520.66	1.26E+08	720	3.14E+06	767	1.19E+07
257.39	1.15E+08	457	9.67E+06	525.8	2.67E+08	721	3.14E+06	768	1.23E+07
258.36	5.45E+08	458	9.67E+06	537.02	6.58E+08	722	3.32E+06	769	1.26E+07
259.52	2.32E+08	459	9.67E+06	542.8	8.20E+07	723	3.32E+06	770	1.28E+07
261.05	2.69E+08	460	1.19E+07	550	1.31E+08	724	3.51E+06	770.41	4.15E+08
262.99	1.28E+07	461	1.19E+07	554.37	6.43E+08	725	3.51E+06	771	1.34E+07
264.24	2.00E+08	462	1.19E+07	558.6	3.48E+08	726	3.51E+06	772	1.37E+07
264.8	1.92E+08	463	1.19E+07	562.8	4.64E+08	727	3.51E+06	773	1.39E+07
270.51	1.60E+08	464	1.19E+07	568.5	2.93E+08	728	3.69E+06	774	1.46E+07
271.99	2.92E+08	465	1.49E+07	572.3	3.90E+08	729	3.69E+06	775	1.46E+07
272.64	5.64E+07	465.22	2.71E+08	580.4	6.29E+07	730	4.06E+06	776	2.60E+07
274.19	3.20E+08	466	1.49E+07	584.33	3.39E+09	731	4.06E+06	776.01	1.50E+07
275.35	1.38E+08	467	1.49E+07	592.4	1.09E+08	732	4.06E+06	777	1.57E+07
275.67	1.15E+08	468	1.86E+07	599.6	1.08E+09	733	4.43E+06	778	1.59E+07
276.15	3.91E+07	469	1.86E+07	609.76	1.00E+09	734	4.43E+06	779	1.61E+07
276.84	4.81E+07	470	1.86E+07	616.6	2.25E+08	735	4.43E+06	780	1.68E+07
277	1.92E+07	471	1.86E+07	624.93	1.35E+09	736	4.62E+06	780.32	2.88E+08
277.27	4.04E+08	472	2.16E+07	629.73	2.28E+09	737	4.62E+06	781	1.70E+07
278.4	1.54E+08	473	2.16E+07	638.5	3.36E+08	738	4.99E+06	782	1.76E+07
281.41	6.73E+07	474	2.45E+07	640.41	7.97E+07	739	4.99E+06	783	1.79E+07
284.15	2.08E+09	475	2.45E+07	640.93	9.45E+07	740	4.99E+06	784	1.83E+07
285.7	9.23E+07	476	2.45E+07	641.81	1.24E+08	741	5.17E+06	785	1.90E+07
289.17	7.56E+07	477	2.83E+07	644.1	1.47E+08	742	5.35E+06	786	1.92E+07
290.69	1.92E+08	478	2.83E+07	650.3	3.89E+07	743	5.35E+06	786.47	3.23E+08
291.7	9.61E+07	479	3.05E+07	657.3	1.54E+07	744	5.54E+06	787	2.01E+07
292.78	2.82E+08	480	3.05E+07	661.4	1.54E+07	745	5.54E+06	787.71	4.20E+08
296.19	3.20E+08	481	3.35E+07	671.5	2.64E+07	746	5.91E+06	788	2.03E+07
299.5	5.57E+07	482	3.35E+07	681.7	9.44E+07	747	6.09E+06	789	2.09E+07
303.31	1.63E+09	483	3.72E+07	685.71	2.52E+08	748	6.28E+06	790	2.12E+07
303.78	8.74E+09	484	4.02E+07	690.8	5.21E+07	749	6.28E+06	790.15	7.22E+08
315.02	1.05E+09	485	4.02E+07	694.3	5.63E+07	750	7.72E+06	791	2.20E+07
316.2	8.84E+08	486	4.31E+07	700	1.85E+06	750.01	8.93E+07	792	2.25E+07
319.01	1.37E+08	487	4.54E+07	701	1.85E+06	751	8.16E+06	793	2.27E+07
319.83	1.15E+09	488	4.91E+07	702	1.85E+06	752	8.16E+06	794	2.36E+07
320.56	3.69E+07	489	4.91E+07	703	2.03E+06	753	8.38E+06	795	2.43E+07
335.41	2.67E+08	489.5	8.18E+07	703.36	4.56E+08	754	8.60E+06	796	2.47E+07
345.13	7.56E+08	490	5.21E+07	704	2.03E+06	755	8.60E+06	797	2.54E+07
345.74	6.60E+08	491	5.50E+07	705	2.03E+06	756	9.04E+06	798	2.62E+07
347.39	1.11E+09	492	5.87E+07	706	2.03E+06	757	9.26E+06	799	2.67E+07
349.85	7.56E+08	493	6.17E+07	707	2.03E+06	758	9.48E+06	800	2.31E+07
356.01	1.77E+09	494	6.40E+07	708	2.03E+06	758.68	7.69E+07	801	2.40E+07
360.8	2.99E+08	495	7.06E+07	709	2.03E+06	759	1.01E+07	802	2.44E+07
364.48	1.29E+09	496	7.36E+07	710	2.40E+06	759.44	5.89E+07	803	2.51E+07
368.07	9.88E+08	497	7.73E+07	711	2.40E+06	760	1.01E+07	804	2.59E+07
399.82	2.67E+08	498	8.03E+07	712	2.40E+06	760.3	2.05E+08	805	2.63E+07

vides generally greater intensities at short wavelengths compared to SERF1, the modeled electron densities using EUV91 were in better agreement with the data in and above the $E-F_1$ region. However, Lyman- β flux from EUV91 produced smaller E -region peak densities than the rocket-measured flux, the latter which provided modeled electron densities in closest agreement with the data.

Siskind *et al.* [1992] have also utilized solar EUV irradiances from EUV91 and SERF1 in a comparative study. The flux from

each model was used as the solar input to a photoelectron model and the resultant modeled photoelectron flux was compared with the Low Altitude Plasma Instrument (LAPI) photoelectron data from the Dynamics Explorer (DE) 2 satellite. They concluded that EUV91 yields an improved fit to the LAPI data as compared to SERF1. However, they also point out that all models still probably underestimate the magnitude of solar flux for wavelengths less than 4 nm.

TABLE 1. (continued)

λ^*	Φ^\dagger	λ	Φ	λ	Φ	λ	Φ	λ	Φ
806	2.70E+07	859	1.15E+08	912	3.93E+08	953	8.89E+06	1003	2.21E+07
807	2.78E+07	860	1.18E+08	913	4.55E+06	954	8.89E+06	1004	2.25E+07
808	2.85E+07	861	1.21E+08	913.99	2.94E+08	955	9.07E+06	1005	2.30E+07
809	2.91E+07	862	1.24E+08	914	4.55E+06	956	9.42E+06	1006	2.34E+07
810	2.98E+07	863	1.27E+08	914.99	2.46E+08	957	9.60E+06	1007	2.38E+07
811	3.07E+07	864	1.30E+08	915	4.55E+06	958	9.78E+06	1008	2.43E+07
812	3.15E+07	865	1.34E+08	915.99	2.18E+08	959	9.96E+06	1009	2.47E+07
813	3.22E+07	866	1.37E+08	916	4.74E+06	960	9.96E+06	1010	2.50E+07
814	3.32E+07	867	1.40E+08	916.99	1.90E+08	961	1.01E+07	1010.2	1.53E+08
815	3.41E+07	868	1.44E+08	917	4.74E+06	962	1.03E+07	1011	2.54E+07
816	3.47E+07	869	1.48E+08	918	5.12E+06	963	1.05E+07	1012	2.59E+07
817	3.56E+07	870	1.51E+08	918.99	1.90E+08	964	1.08E+07	1013	2.66E+07
818	3.63E+07	871	1.55E+08	919	5.12E+06	965	1.10E+07	1014	2.70E+07
819	3.76E+07	872	1.59E+08	920	5.31E+06	966	1.12E+07	1015	2.75E+07
820	3.82E+07	873	1.63E+08	920.96	2.18E+08	967	1.16E+07	1016	2.79E+07
821	3.95E+07	874	1.68E+08	921	5.31E+06	968	1.17E+07	1017	2.84E+07
822	4.04E+07	875	1.72E+08	922	5.31E+06	969	1.19E+07	1018	2.90E+07
823	4.15E+07	876	1.76E+08	923	5.69E+06	970	1.21E+07	1019	2.95E+07
824	4.27E+07	877	1.80E+08	923.15	2.27E+08	971	1.23E+07	1020	3.01E+07
825	4.36E+07	878	1.85E+08	924	5.69E+06	972	1.24E+07	1021	3.06E+07
826	4.47E+07	879	1.90E+08	925	5.87E+06	972.54	1.47E+09	1022	3.11E+07
827	4.60E+07	880	1.95E+08	926	5.87E+06	973	1.26E+07	1023	3.17E+07
828	4.69E+07	881	2.00E+08	926.2	2.37E+08	974	1.28E+07	1024	3.20E+07
829	4.82E+07	882	2.05E+08	927	6.06E+06	975	1.32E+07	1025	3.29E+07
830	4.96E+07	883	2.10E+08	928	6.06E+06	976	1.35E+07	1025.72	1.18E+10
831	5.07E+07	884	2.15E+08	929	6.25E+06	977	1.39E+07	1026	3.35E+07
832	5.20E+07	885	2.21E+08	930	6.25E+06	977.02	1.04E+10	1027	3.40E+07
833	5.35E+07	886	2.26E+08	930.75	2.46E+08	978	1.40E+07	1028	3.47E+07
834	5.46E+07	887	2.32E+08	931	6.44E+06	979	1.42E+07	1029	3.55E+07
834.2	1.24E+09	888	2.38E+08	932	6.44E+06	980	1.46E+07	1030	3.60E+07
835	5.63E+07	889	2.44E+08	933	6.63E+06	981	1.48E+07	1031	3.65E+07
836	5.74E+07	890	2.50E+08	933.38	1.86E+08	982	1.49E+07	1031.91	7.66E+09
837	5.89E+07	891	2.57E+08	934	6.63E+06	983	1.51E+07	1032	3.73E+07
838	6.04E+07	892	2.63E+08	935	6.82E+06	984	1.56E+07	1033	3.78E+07
839	6.20E+07	893	2.70E+08	936	6.82E+06	985	1.58E+07	1034	3.87E+07
840	6.35E+07	894	2.76E+08	937	7.01E+06	986	1.60E+07	1035	3.94E+07
841	6.54E+07	895	2.83E+08	937.8	3.60E+08	987	1.64E+07	1036	4.00E+07
842	6.67E+07	896	2.91E+08	938	7.20E+06	988	1.65E+07	1036.34	7.52E+08
843	6.86E+07	897	2.98E+08	939	7.20E+06	989	1.71E+07	1037	4.07E+07
844	7.02E+07	898	3.05E+08	940	7.39E+06	989.79	3.40E+08	1037.02	8.46E+08
845	7.21E+07	899	3.13E+08	941	7.39E+06	990	1.72E+07	1037.61	3.07E+09
846	7.40E+07	900	2.91E+08	942	7.77E+06	991	1.78E+07	1038	4.16E+07
847	7.58E+07	901	2.98E+08	943	8.15E+06	991.55	6.80E+08	1039	4.23E+07
848	7.77E+07	902	3.06E+08	944	8.15E+06	992	1.80E+07	1040	4.32E+07
849	7.95E+07	903	3.14E+08	944.52	1.23E+08	993	1.83E+07	1041	4.37E+07
850	9.16E+07	904	3.22E+08	945	8.34E+06	994	1.85E+07	1042	4.46E+07
851	9.42E+07	904.1	2.22E+08	946	8.53E+06	995	1.88E+07	1043	4.55E+07
852	9.65E+07	905	3.30E+08	947	8.53E+06	996	1.92E+07	1044	4.63E+07
853	9.92E+07	906	3.38E+08	948	8.72E+06	997	1.94E+07	1045	4.70E+07
854	1.01E+08	907	3.47E+08	949	8.91E+06	998	2.01E+07	1046	4.81E+07
855	1.04E+08	908	3.56E+08	949.74	6.63E+08	999	2.04E+07	1047	4.88E+07
856	1.07E+08	909	3.64E+08	950	8.36E+06	1000	2.11E+07	1048	4.97E+07
857	1.10E+08	910	3.74E+08	951	8.54E+06	1001	2.12E+07	1049	5.04E+07
858	1.12E+08	911	3.83E+08	952	8.71E+06	1002	2.16E+07	1050	0.00E+00

Read 7.22E+05 as 7.22×10^5 .

* Wavelength in Å.

† Flux in photons $\text{cm}^{-2} \text{s}^{-1}$

DISCUSSION

There are a number of basic requirements for full-disk empirical EUV irradiance models. The models must have wavelength representations of discrete lines, continua, and intervals which are compatible with user requirements. The models must demonstrate consistency between their results and the data sets for all periods of solar activity. Several physical phenomena must be repro-

ducible by the models, including solar cycle (11-year) magnitude, phase, rise, and decline, solar rotation (27-day) magnitude and phase, and differences in emissions from specific solar regions and features. Our current understanding of physics should be represented in the models, i.e., accuracy in continua and line shapes. Finally, the models should allow easy application to special cases such as solar minimum, solar maximum, and campaign dates.

In order to improve substantially on current models, work is

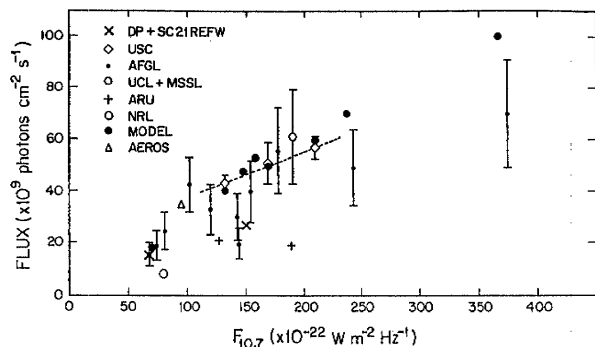


Fig. 9. The total integrated solar EUV flux from 5 to 57.5 nm adapted from *Ogawa et al.* [1990]. Organizations that made individual rocket measurements are described in that reference. The USC data have the lowest uncertainty and are denoted by diamonds. The model values for a variety of levels of solar activity, as indicated by $F_{10.7}$ in the abscissa, are shown as filled circles with no error bars. Additional data points have been added: the AEROS A satellite measurement on January 19, 1973, when $F_{10.7} = 95$, which had an integrated flux of $34.6 \times 10^9 \text{ ph cm}^{-2} \text{ s}^{-1} \pm 20\%$ described by *Schmidtke* [1976]; the *Donnelly and Pope* [1973] (DP) integrated flux; and the SC#21REFW integrated flux. The integrated fluxes for the two latter spectra are $26.9 \times 10^9 \text{ ph cm}^{-2} \text{ s}^{-1}$ ($F_{10.7} = 150$) and $15.0 \times 10^9 \text{ ph cm}^{-2} \text{ s}^{-1}$ ($F_{10.7} = 68$), respectively. They are denoted by a cross on the figure.

needed in several areas. The primary goal is to obtain regular, consistent measurements above the atmosphere with high photometric accuracy over a substantial part of the solar cycle. Far and above anything else, these measurements improve solar EUV modeling. For example, one area is that there still have not been unambiguous full-disk measurements over a full solar cycle with a set of calibrated or intercalibrated instruments. A second area, instrument calibration, is an issue addressed by *Neupert* [1986], *Schmidtke* [1992], and *Parkinson et al.* [1992]. For a third area, one notes that within and between the existing satellite data sets there are gaps. Fourthly, not all usable data sets have been incorporated into the present models. Finally, a comparison of the AE-E and San Marco data sets for the ascending phase of the solar cycle, exemplified by work started by *Schmidtke et al.* [1993], is useful to better understand the solar variations in solar cycle phases.

There are also secondary areas of work within the context of obtaining more data that improve solar EUV modeling. For example, long-term data with high spectral, temporal, and spatial resolution throughout the EUV are needed. Combined spectral, temporal, and spatial resolution allows the incorporation of solar physics into models. This results from connecting the irradiance variations to solar feature evolution (e.g., active regions, network emission, loops, and holes) and to center-to-limb functions. These irradiances differ from background or full-disk emissions.

Spectral resolution much less than 0.1 nm allows line shapes to be modeled and species' temperatures over defined altitude regions to be determined. Higher spectral resolution measurements of full-disk emissions allows higher resolution distinctions between chromospheric and coronal lines that are spectrally close to one another such as He II 30.378 nm and Si XI 30.331 nm lines. Higher resolution allows the differentiation of weak emission lines from nearby continua emissions. Finer spectral resolution also as-

sists the development of spectrum formats with highly defined line binning. An example of this is in the region of $0.1 < 3 \text{ nm}$ where several inner shell electron ionization thresholds exist. Higher resolution wavelength binning is possible with better known atmospheric constituent absorption cross sections [Conway, 1988]. S. C. Solomon (private communication, 1992) suggests a refinement of the wavelength binning format used in SERF1 and EUV91 encompassing 95 wavelength intervals including the brighter emission features and continuum intervals between 0.1 and 205 nm.

Temporal resolution of the order of minutes allows periodic helioseismic and flare activity to be modeled. Spatial resolution on the arcsec level allows investigation and modeling of the small- and medium-scale dynamics of the solar subsurface, photosphere, and atmospheric layers based upon their deviations from the solar "climatological" norms. Current developments in imaging technology strongly encourage these studies in solar physics.

From an aeronomical perspective, there are important solar EUV questions to be resolved. For example, during solar cycle minimum conditions should an EUV flux value be used for the 5 to 57.5 nm total integrated flux that is higher than irradiances measured by rockets in the 1970s? *Richards and Torr* [1984], *Ogawa and Judge* [1986], *Link et al.* [1988], and *Winningham et al.* [1989] suggest that some or all of the total flux in that wavelength range be higher during low solar activity by up to a factor of 2. Either the entire range of 5 to 57.5 nm should have greater flux or the shorter wavelengths should vary more dramatically than those variations presently modeled. In the latter scenario the total flux of 5 to 57.5 nm remains approximately the same. The longer wavelengths contribute the bulk of the measured photons while the shorter wavelengths provide more secondary ionization energy into the lower thermosphere. Inclusion of the AEROS B [Schmidtke et al., 1974; Schmidtke, 1979] and SOLRAD [Kreplin, 1970; Kreplin et al., 1977; Kahler and Kreplin, 1991; Kreplin and Horan, 1992] data in EUV models will potentially answer that question. These data, which are archived with the NSSDC (AEROS B) or need to be digitized (R. Kreplin, private communication, 1991), have not yet been included in contemporary EUV models. Soviet Prognoz data may also aid in this research as would combined ionization cell and spectrographic EUV measurements during solar minimum conditions in the mid-1990s.

A corollary question is whether or not a value for the soft X rays ($0.1 < 10 \text{ nm}$) should be used which is substantially higher by more than an order of magnitude at all levels of solar activity? *Barth et al.* [1988] and *Siskind et al.* [1990] suggest from lower thermospheric nitric oxide (NO) data and model comparisons that these soft X rays should be scaled upwards significantly (up to 60 times). Inclusion into EUV models of the SOLRAD data and the new YOKHOH data binned into full-disk values may provide an answer.

Another question can be posed. Can the EUV irradiances that produce F- and E-region ionization be estimated with better absolute accuracy? Measured electron densities are still higher by 30 to 50% or more, depending upon date, compared to state-of-the-art ionospheric model calculations (PRIMO workshop, 1991 CEDAR meeting; M. Buonsanto, private communication, 1991). Even slight increases in solar EUV irradiance values of the order of 5 to 10% would contribute to a clearer understanding of ionospheric variability if this flux were to have less uncertainty than the solar data that are presently used. The low, moderate, and high solar activity measurements by the AEROS A/B, SOLRAD, and San Marco satellites, combined with recent and pending solar rocket measurements (T. N. Woods, H. Ogawa, and S. Chakrabarti, private communications, 1991) will potentially improve ionospheric

modeling by constraining the solar Lyman- β and the soft X rays to more accurate irradiance values. There are new techniques to estimate Lyman- β flux through proxy use [Bouwer, 1992] which additionally may help constrain the range of energy input to the E-region for peak ionization modeling and which have not yet been included in EUV models.

Another aeronomically important task is the extension of EUV models into the FUV to connect with existing data sets from the Solar Mesosphere Explorer (SME) and Upper Atmosphere Research Satellite (UARS) and to overlap with UV empirical models. Of particular interest in the FUV are important discrete lines like 121.6 nm (H I) and 130.4 nm (O I) as well as the Schumann-Runge continuum and bands.

Some contemporary solar EUV models use multiple linear regression techniques to correlate the independent proxy data sets with the EUV data sets, thus allowing the opportune inclusion of new proxy or EUV data as they become available. However, there may be other techniques for modeling the irradiance variations that have not yet been investigated. Nusinov [1984, 1992] used nonlinear regression formulas that provide an interesting step in this direction.

New proxy candidates for chromospheric emissions (6000–10,000 K) include space-based observations of He I (58.4 nm), He II (30.4 nm if it can be resolved from the Si XI line), and Mg II (c/w) along with the ground-based observations of Ca II K plage and Ca K 0.1-nm index. These candidates complement the Lyman- α and He I 1083-nm EW proxies presently being used. New proxy candidates for transition region irradiance ($T > 20,000$ K) include space-based observations of Fe IX (16.9–17.3 nm) and Fe XI (18 nm). A candidate irradiance proxy of the low-temperature ($T = 1 \times 10^6$ K) coronal emission is the space-based observation of Fe XIII (20–20.4 nm). Hot coronal irradiance proxy candidates (2 or 3×10^6 K) include the space-based 0.1 to 0.8 nm X rays and the Fe XV (28.4 nm) along with the ground-based coronagraph observations of the Fe XIV (530.3 nm) green line. The transition region and coronal candidates complement the present $F_{10.7}$ daily and 81-day mean value ground-observed data. R. F. Donnelly (private communication, 1991) has indicated that SERF3 will take advantage of many of these new proxies.

Important improvements in empirical models may incorporate more physical processes into the irradiance variations. For example, the provision of the theoretical solar blackbody continuum that underlies the line emission is important for those parts of the spectrum where few lines are prominent. This theoretical contribution to empirical models might first occur through the incorporation of the He I, Lyman, and C I continua slopes and magnitudes.

There are other long-term objectives for developing accurate solar EUV empirical models in addition to the need for understanding fundamental solar physics and solar-terrestrial energy coupling. For example, accurate modeling capabilities fulfill future aerospace requirements. Those requirements anticipate daily or hourly full-disk predicted EUV irradiance values to be utilized for satellite operational purposes.

A current major goal of STEP is to advance the quantitative understanding of the coupling mechanisms responsible for the transfer of energy and mass between regions of the solar-terrestrial system. Solar EUV irradiance modeling which is linked to ionospheric and upper atmospheric modeling continues to be an important element of that study. The culmination of the current stage of empirical EUV modeling refinements is an EUV component of a COSPAR international reference solar model. This activity is coordinated within the goals of the Solar Electromagnetic Radiation Study for Solar Cycle 22 (SOLERS22).

SUMMARY

Empirical solar EUV irradiance modeling, starting with empirical solar blackbody function fitting, has progressed through fudge factors and reference spectra to multiple linear correlations using sparse data sets. After four decades of rocket and satellite measurements that provided typical (or reference) fluxes and time series measurements, three independently derived empirical models were completed by the beginning of the 1990s. These are Hinteregger's 1981 SERF1, Nusinov's 1984 two-component, and Tobiska's 1990/1991 SERF2/EUV91 models that provide daily full-disk flux values from 2 to 105 nm at 1 AU. The models followed, or were coincident with, the development of four reference spectra. These latter spectra were the Hinteregger EUV flux standard in 1965 for quiet solar conditions, the Donnelly and Pope moderate solar activity spectrum in 1973, the Hinteregger SC#21REFW solar minimum reference spectrum in 1981, and the Schmidtke ASSI reference spectrum for moderate solar activity in 1992.

Efforts to refine EUV models are still in progress. Issues currently being considered include finer spectral, temporal, and spatial resolution within the context of obtaining regular and accurate EUV flux measurements. More complete use of existing full-disk data sets is also contemplated where temporal and spectral gaps in existing models can be filled in. Atmospheric and ionospheric modeling, with its use of modeled solar EUV irradiances, provides an integrity check for the solar models. The solar models, with some of the proposed revisions, can answer several important questions related to solar-terrestrial coupling. In particular, questions related to secondary ionization, NO production, and E-region peak densities can be addressed with models which incorporate the contemplated revisions. Proposed extensions of EUV models into the FUV provide the basis for self-consistent solar irradiance modeling useful for aeronautical applications. Improved EUV models will advance our understanding of the fundamental coupling of energetics in the Sun-Earth system and will provide the foundation for a new generation of operational and prediction models at the turn of the century.

Acknowledgments. The author appreciates the support given by the TELOS Systems Group for this work.

The Editor thanks G. J. Rottman and R. F. Donnelly for their assistance in evaluating this paper.

REFERENCES

- Barth, C. A., W. K. Tobiska, D. E. Siskind, and D. D. Cleary, Solar-terrestrial coupling: Low-latitude thermospheric nitric oxide, *Geophys. Res. Lett.*, **15**, 92–94, 1988.
- Barth, C. A., W. K. Tobiska, G. J. Rottman, and O. R. White, Comparison of 10.7-cm radio flux with SME solar Lyman alpha flux, *Geophys. Res. Lett.*, **17**, 571–574, 1990.
- Baum, W. A., F. S. Johnson, J. J. Oberly, C. C. Rockwood, C. V. Strain, and R. Tousey, Solar ultraviolet spectrum to 88 kilometers, *Phys. Rev.*, **70**, 781–782, 1946.
- Bruevich, E. A., and A. A. Nusinov, Spectrum of short-wavelength radiation for aeronomic calculations at various solar activity levels, *Geomagn. Aeron.*, **24**, 478–481, 1984.
- Bouwer, S. D., A suggested proxy index for estimating solar Lyman- β , in *Proceedings of the Workshop on the Solar Electromagnetic Radiation Study for Solar Cycle 22*, edited by R. F. Donnelly, pp. 371–382, Space Environment Laboratory, National Oceanic and Atmospheric Administration Environmental Research Laboratory, Boulder, Colo., 1992.

- Buonsanto, M. J., S. C. Solomon, and W. K. Tobiska, Comparison of measured and modeled solar EUV flux and its effect on the E-F1 region ionosphere, *J. Geophys. Res.*, **97**, 10,513-10,524, 1992.
- Carlson, R. W., H. S. Ogawa, E. Phillips, and D. L. Judge, Absolute measurement of the extreme UV solar flux, *Appl. Opt.*, **23**, 2327-2332, 1984.
- Chapman, S., Some phenomena of the upper atmosphere (Bakerian Lecture), *Proc. R. Soc., London, Ser. A*, **132**, 353-374, 1931.
- Chapman, R. D., and W. M. Neupert, Slowly varying component of extreme ultraviolet solar radiation and its relation to solar radio radiation, *J. Geophys. Res.*, **79**, 4138-4148, 1974.
- Conway, R. R., Photoabsorption and photoionization cross sections of O, O₂, and N₂ for photoelectron production calculations: A compilation of recent laboratory measurements, *Memo. Rep. 6155*, Nav. Res. Lab., Washington, D. C., 1988.
- Covington, A. E., Solar noise observations on 10.7 centimeters, *Proc. IRE*, **36**, 454-457, 1948.
- Donnelly, R. F., SMS-GOES solar soft X-ray measurements, Part I, SMS-1, SMS-2, and GOES-1 measurements from July 1, 1974, through December 31, 1976, *Tech. Memo. ERL SEL-56*, National Oceanic and Atmospheric Administration, Boulder, Colo., 1981.
- Donnelly, R. F., Comparison of nonflare solar soft X-ray flux with 10.7-cm radio flux, *J. Geophys. Res.*, **87**, 6331-6334, 1982.
- Donnelly, R. F., Gaps between solar UV & EUV radiometry and atmospheric sciences, in *Solar Radiative Output Variation*, edited by P. Foukal, pp. 139-142, Cambridge Research and Instrumentation, Cambridge, Mass., 1987a.
- Donnelly, R. F., Temporal trends of solar EUV and UV full-disk fluxes, *Sol. Phys.*, **109**, 37-58, 1987b.
- Donnelly, R. F., Solar Electromagnetic Radiation Flux Study (SERFS) for the World Ionosphere-Thermosphere Study (WITS), in *World-Ionosphere/Thermosphere Study WITS Handbook*, edited by C. H. Liu and B. Edwards, pp. 201-207, Vol. 1, SCOSTEP Secretariat, University of Illinois, Urbana, Ill., 1988a.
- Donnelly, R. F., The solar UV Mg II core-to-wing ratio from the NOAA 9 satellite during the rise of solar cycle 22, *Adv. Space Res.*, **8**, 77-80, 1988b.
- Donnelly, R. F., and J. H. Pope, The 1-3000 Å solar flux for a moderate level of solar activity for use in modeling the ionosphere and upper atmosphere, *Tech. Rep. ERL 276-SEL 25*, National Oceanic and Atmospheric Administration, Boulder, Colo., 1973.
- Donnelly, R. F., and S. D. Bouwer, SMS-GOES solar soft X-ray measurements Part II. SMS-2, GOES-1, GOES-2 and GOES-3 measurements from January 1, 1977, through December 31, 1980, *Tech. Memo. ERL SEL-57*, National Oceanic and Atmospheric Administration, Boulder, Colo., 1981.
- Donnelly, R. F., D. F. Heath, J. L. Lean, and G. J. Rottman, Differences in the temporal variations of solar UV flux, 10.7-cm solar radio flux, sunspot number, and Ca-K plage data caused by solar rotation and active region evolution, *J. Geophys. Res.*, **88**, 9883-9888, 1983.
- Donnelly, R. F., J. W. Harvey, D. F. Heath, and T. P. Repoff, Temporal characteristics of the solar UV flux and He I line at 1083 nm, *J. Geophys. Res.*, **90**, 6267-6273, 1985.
- Donnelly, R. F., H. E. Hinteregger, and D. F. Heath, Temporal variations of solar EUV, UV, and 10830-Å radiations, *J. Geophys. Res.*, **91**, 5567-5578, 1986a.
- Donnelly, R. F., L. C. Puga, and W. S. Busby, Temporal characteristics of solar EUV, UV and 10830-Å full-disk fluxes, *Tech. Memo. ERL ARL-146*, National Oceanic and Atmospheric Administration, Silver Spring, Md., 1986b.
- Donnelly, R. F., and L. C. Puga, Thirteen-day periodicity and the center-to-limb dependence of UV, EUV, and X-ray emission of solar activity, *Sol. Phys.*, **130**, 369-390, 1990.
- Feng, W., H. S. Ogawa, and D. L. Judge, The absolute solar soft x-ray flux in the 20-100 Å region, *J. Geophys. Res.*, **94**, 9125-9130, 1989.
- Fontenla, J. M., E. H. Avrett, and R. Loeser, Energy balance in the solar transition region. I. Hydrostatic thermal models with ambipolar diffusion, *Ap. J.*, **355**, 700-718, 1990.
- Fontenla, J. M., E. H. Avrett, and R. Loeser, Energy balance in the solar transition region. II. Effects of pressure and energy input on hydrostatic models, *Ap. J.*, **377**, 712-725, 1991.
- Gelfreikh, G. B., Solar radio emission at centimeter wavelengths, in *Proceedings of the Workshop on the Solar Electromagnetic Radiation Study for Solar Cycle 22*, edited by R. F. Donnelly, pp. 196-227, Space Environment Laboratory, National Oceanic and Atmospheric Administration Environmental Research Laboratory, Boulder, Colo., 1992.
- Hall, L. A., K. R. Damon, and H. E. Hinteregger, Solar extreme ultraviolet photon flux measurements in the upper atmosphere of August 1961, in *Space Res.*, Vol. III, edited by W. Priester, pp. 745-759, John Wiley, New York, 1963.
- Hall, L. A., and H. E. Hinteregger, Solar radiation in the extreme ultraviolet and its variation with solar rotation, *J. Geophys. Res.*, **75**, 6959-6965, 1970.
- Harvey, J., Helium 10830 Å irradiance: 1975-1983, in *Solar Irradiance Variations on Active Region Time Scales*, edited by B. LaBonte, G. Chapman, H. Hudson, and R. Wilson, NASA Conf. Publ., CP-2310, 197-211, 1984.
- Heath, D. F., and B. M. Schlesinger, The Mg 280 nm doublet as a monitor of changes in Solar ultraviolet irradiance, *J. Geophys. Res.*, **91**, 8672-8682, 1986.
- Hedin, A. E., Correlations between thermospheric density and temperature, solar EUV flux, and 10.7-cm flux variations, *J. Geophys. Res.*, **89**, 9828-9834, 1984.
- Heroux, L., and H. E. Hinteregger, Aeronomical reference spectrum for solar UV below 2000 Å, *J. Geophys. Res.*, **83**, 5305-5308, 1978.
- Hinteregger, H. E., Interplanetary ionization by solar extreme ultraviolet radiation, *Ap. J.*, **132**, 801-811, 1960.
- Hinteregger, H. E., Effects of solar XUV radiation on the Earth's atmosphere, in *Annals of the IQSY*, Vol. 5, edited by A. C. Strickland, pp. 305-322, MIT Press, Cambridge, Mass., 1969.
- Hinteregger, H. E., The extreme ultraviolet solar spectrum and its variation during a solar cycle, *Ann. Geophys.*, **26**, 547-554, 1970.
- Hinteregger, H. E., EUV fluxes in the solar spectrum below 2000 Å, *J. Atmos. Terr. Phys.*, **38**, 791-806, 1976.
- Hinteregger, H. E., L. A. Hall, and G. Schmidtke, Solar XUV radiation and neutral particle distribution in July 1963 thermosphere, *Space Res.*, **V**, 1175-1190, 1965.
- Hinteregger, H. E., K. Fukui, and B. R. Gilson, Observational, reference and model data on solar EUV, from measurements on AE-E, *Geophys. Res. Lett.*, **8**, 1147-1150, 1981.
- Ivanov-Kholodny, G. S. and T. V. Kazachevskaya, Variations in the integral EUV solar flux during the solar activity maximum from Prognoz satellite measurements, in *International Solar Maximum Year Workshop, Proceedings of an International Workshop*, Vol. II, pp. 39-44, Academy of Sciences of the USSR, Institute of Terrestrial Magnetism, Ionosphere and Radio Wave Propagation, Simferopol, 1981.
- Jacchia, L. G., Two atmospheric effects in the orbital acceleration of artificial satellites, *Nature*, **183**, 526-527, 1958.
- Kahler, S. W., A comparison of the SMS/GOES and SOLRAD X-

- ray detectors for quiet-sun studies, in *Proceedings of the Workshop on the Solar Electromagnetic Radiation Study for Solar Cycle 22*, edited by R. F. Donnelly, pp. 426-439, Space Environment Laboratory, National Oceanic and Atmospheric Administration Environmental Research Laboratory, Boulder, Colo., 1992.
- Kahler, S. W., and R. W. Kreplin, The NRL SOLRAD X-ray detectors: A summary of the observations and a comparison with the SMS/GOES detectors, *Sol. Phys.*, **133**, 371-384, 1991.
- Kazachevskaya, T. V., G. S. Ivanov-Kholodny, and D. A. Gonyukh, On the estimation of the absolute value of the flux of short-wave radiation of the Sun by measurements of satellites in 1978-79, *Geomagn. Aeron.*, **25**, 995-997, 1985.
- Kazachevskaya, T. V., L. L. Bukusova, D. A. Gonyukh, A. I. Lomovsky, and Yu. N. Tsygelnitsky, E.U.V. observations of solar flares from Mars, *Planet. Space Sci.*, **39**, 39-40, 1991.
- Kazachevskaya, T. V., and A. I. Lomovsky, Solar EUV flux as measured in 1978-79 and 1988-89 using a thermoluminescent technique, in *Proceedings of the Workshop on the Solar Electromagnetic Radiation Study for Solar Cycle 22*, edited by R. F. Donnelly, pp. 319-326, Space Environment Laboratory, National Oceanic and Atmospheric Administration Environmental Research Laboratory, Boulder, Colo., 1992.
- Keil, S. L., and S. P. Worden, Variations in the solar Calcium K line, *Ap. J.*, **276**, 766-781, 1984.
- Kelly, R. L., Atomic emission lines below 2000 Angstroms, hydrogen through argon, *NRL Rep. 6648*, Nav. Res. Lab., Washington, D. C., 1968.
- Kreplin, R. W., The solar cycle variation of soft X-ray emission, *Ann. Geophys.*, **26**, 567-574, 1970.
- Kreplin, R. W., K. P. Dere, D. M. Horan, and J. F. Meekins, The solar spectrum below 10 Å, in *The Solar Output and Its Variation*, edited by O. R. White, pp. 287-312, Colorado Associated University Press, Boulder, Colo., 1977.
- Kreplin, R. W., and D. M. Horan, Variability of X-ray and EUV solar radiation in solar cycles 20 and 21, in *Proceedings of the Workshop on the Solar Electromagnetic Radiation Study for Solar Cycle 22*, edited by R. F. Donnelly, pp. 405-425, Space Environment Laboratory, National Oceanic and Atmospheric Administration Environmental Research Laboratory, Boulder, Colo., 1992.
- Kurucz, R. L., The solar spectrum, in *The Solar Interior and Atmosphere*, edited by A. N. Cox, W. C. Livingston, and M. Matthews, pp. 663-669, University of Arizona Press, Tucson, 1991.
- Lean, J. L., Solar ultraviolet irradiance variations: A review, *J. Geophys. Res.*, **92**, 839-868, 1987.
- Lean, J., Solar EUV irradiances and indices, *Adv. Space Res.*, **8**, 263-292, 1988.
- Lean, J., A comparison of models of the Sun's extreme ultraviolet irradiance variations, *J. Geophys. Res.*, **95**, 11,933-11,944, 1990.
- Lean, J. L., and A. Skumanich, Variability of the Lyman alpha flux with solar activity, *J. Geophys. Res.*, **88**, 5751-5759, 1983.
- Link, R., G. R. Gladstone, S. Chakrabarti, and J. C. McConnell, A reanalysis of rocket measurements of the ultraviolet dayglow, *J. Geophys. Res.*, **93**, 14,631-14,648, 1988.
- Linsky, J. L., The solar output and variability viewed in the broader context of stellar activity, in *The Solar Output and Its Variation*, edited by O. R. White, pp. 477-515, Colorado Associated University Press, Boulder, Colo., 1977.
- Neupert, W. M., The solar corona above active regions: A comparison of extreme ultraviolet line emission with radio emission, *Sol. Phys.*, **2**, 294-315, 1967.
- Neupert, W. M., Problems and approaches to the calibration of solar EUV instrumentation in space, *SPIE X-Ray Calibration: Techniques, Sources, and Detectors*, **689**, 224-230, 1986.
- Neupert, W. M., Spatial correlation, of solar extreme ultraviolet and microwave emission and implications for improved EUV proxies, in *Proceedings of the Workshop on the Solar Electromagnetic Radiation Study for Solar Cycle 22*, edited by R. F. Donnelly, pp. 360-370, Space Environment Laboratory, National Oceanic and Atmospheric Administration Environmental Research Laboratory, Boulder, Colo., 1992.
- Neupert, W. M., W. E. Behring, and J. C. Lindsay, The solar spectrum from 50 Å to 400 Å, *Space Res.*, **IV**, 719-729, 1964.
- Nusinov, A. A., Dependence of the intensity of lines of short-wavelength solar radiation on the solar activity level, *Geomagn. Aeron.*, **24**, 439-444, 1984.
- Nusinov, A. A., Models for prediction of EUV- and X-ray solar radiation based on 10.7-cm radio emission, in *Proceedings of the Workshop on the Solar Electromagnetic Radiation Study for Solar Cycle 22*, edited by R. F. Donnelly, pp. 354-359, Space Environment Laboratory, National Oceanic and Atmospheric Administration Environmental Research Laboratory, Boulder, Colo., 1992.
- Ogawa, H. S., and D. L. Judge, Absolute solar flux measurement shortward of 575 Å, *J. Geophys. Res.*, **91**, 7089-7092, 1986.
- Ogawa, H. S., L. R. Canfield, D. McMullin, and D. L. Judge, Sounding rocket measurement of the absolute solar EUV flux utilizing a silicon photodiode, *J. Geophys. Res.*, **95**, 4291-4295, 1990.
- Parkinson, W. H., P. L. Smith, and G. Schmidtke, Absolute, extreme-ultraviolet, solar spectral irradiance monitors, in *Proceedings of the Workshop on the Solar Electromagnetic Radiation Study for Solar Cycle 22*, edited by R. F. Donnelly, pp. 332-337, Space Environment Laboratory, National Oceanic and Atmospheric Administration Environmental Research Laboratory, Boulder, Colo., 1992.
- Planck, M., On the theory of thermal radiation, *Ann. Phys.*, **4**, 553-563, 1901.
- Richards, P. G., and D. G. Torr, An investigation of the consistency of the ionospheric measurements of the photoelectron flux and solar EUV flux, *J. Geophys. Res.*, **89**, 5625-5635, 1984.
- Roble, R. G., Solar cycle variation of the global mean structure of the thermosphere, in *Solar Radiative Output Variation*, edited by P. Foukal, pp. 1-24, Cambridge Research and Instrumentation, Cambridge, Mass., 1987.
- Roble, R. G., and G. Schmidtke, Calculated ionospheric variations due to changes in the solar EUV flux measured by the AEROS spacecraft, *J. Atmos. Terr. Phys.*, **41**, 153-160, 1979.
- Roemer, M., W. Framke, and K. G. H. Schuchardt, Solar EUV and decimetric indices and thermospheric models, *Adv. Space Res.*, **3**, 75-82, 1983.
- Rottman, G. J., Results from space measurements of solar UV and EUV flux, in *Solar Radiative Output Variation*, edited by P. Foukal, pp. 71-86, Cambridge Research and Instrumentation, Cambridge, Mass., 1987.
- Rottman, G. J., Observations of solar UV and EUV variability, *Adv. Space Res.*, **8**, 53-66, 1988.
- Rusin, V., and M. Rybansky, Ground-based coronal indices, in *Proceedings of the Workshop on the Solar Electromagnetic Radiation Study for Solar Cycle 22*, edited by R. F. Donnelly, pp. 168-190, Space Environment Laboratory, National Oceanic and Atmospheric Administration Environmental Research Laboratory, Boulder, Colo., 1992.
- Rybansky, M., and V. Rusin, Coronal index of solar activity in the

- years 1988 and 1989, in *Proceedings of the Workshop on the Solar Electromagnetic Radiation Study for Solar Cycle 22*, edited by R. F. Donnelly, pp. 191-195, Space Environment Laboratory, National Oceanic and Atmospheric Administration Environmental Research Laboratory, Boulder, Colo., 1992.
- Saha, M. N., On the action of ultra-violet sunlight upon the upper atmosphere, *Proc. R. Soc., London, Ser. A*, 160, 155-173, 1937.
- Schmidtke, G., EUV indices for solar-terrestrial relations, *Geophys. Res. Lett.*, 3, 573-576, 1976.
- Schmidtke, G., The AEROS EUV measurements, *J. Geomagn. Geoelectr. Suppl.*, 31, 81-84, 1979.
- Schmidtke, G., Modelling of the solar extreme ultraviolet irradiance for aeronomic applications, in *Handbuch der Physik*, Vol. XLIX/7, Geophysics III, Part VII, edited by S. Flugge, pp. 1-55, Springer-Verlag, Berlin, 1984.
- Schmidtke, G., Observations of the solar EUV spectral irradiance, in *Proceedings of the Workshop on the Solar Electromagnetic Radiation Study for Solar Cycle 22*, edited by R.F. Donnelly, pp. 303-318, Space Environment Laboratory, National Oceanic and Atmospheric Administration Environmental Research Laboratory, Boulder, Colo., 1992.
- Schmidtke, G., W. Schweizer, and M. Knothe, The AEROS-EUV spectrometer, *J. Geophys.*, 40, 577-584, 1974.
- Schmidtke, G., P. Seidl, and C. Wita, Airglow-solar spectrometer instrument (20-700 nm) aboard the San Marco D/L satellite, *Appl. Opt.*, 24, 3206-3213, 1985.
- Schmidtke, G., T. N. Woods, J. Worden, G. J. Rottman, H. Doll, C. Wita, and S. C. Solomon, Solar EUV irradiance from the San Marco ASSI: A reference spectrum, *Geophys. Res. Lett.*, 19, 2175-2178, 1992.
- Schmidtke, G., H. Doll, and C. Wita, Measurement of solar EUV/UV radiation of the steeply rising solar cycle 22 during the San Marco 5 mission and proposed instrumentation to achieve high radiometric accuracy, *Adv. Space Res.*, 13, (1)221-246, 1993.
- Simon, P. C., and W. K. Tobiska, Solar EUV irradiance variations: A review, *J. Geomagn. Geoelectr. Suppl.*, 43, 823-833, 1991.
- Siskind, D. E., C. A. Barth, and D. D. Cleary, The possible effect of solar soft X rays on thermospheric nitric oxide, *J. Geophys. Res.*, 95, 4311-4317, 1990.
- Siskind, D. E., S. C. Solomon, J. U. Kozyra, and J. D. Winningham, Inferring the temporal variability of the solar soft X-ray flux, in *Proceedings of the Workshop on the Solar Electromagnetic Radiation Study for Solar Cycle 22*, edited by R. F. Donnelly, pp. 445-459, Space Environment Laboratory, National Oceanic and Atmospheric Administration Environmental Research Laboratory, Boulder, Colo., 1992.
- Spruit, H. C., Influence of magnetic activity on the solar luminosity and radius, in *Solar Radiative Output Variation*, edited by P. Foukal, pp. 254-288, Cambridge Research and Instrumentation, Cambridge, Mass., 1987.
- Tapping, K. F., Recent solar radio astronomy at centimeter wavelengths: The temporal variability of the 10.7-cm flux, *J. Geophys. Res.*, 92, 829-838, 1987.
- Timothy, J. G., The solar spectrum between 300 and 1200 Å, in *The Solar Output and Its Variation*, edited by O. R. White, pp. 133-150, Colorado Associated University Press, Boulder, Colo., 1977.
- Tobiska, W. K., A solar extreme ultraviolet flux model, Ph.D. thesis, Univ. of Colo., Boulder, 1988.
- Tobiska, W. K., SERF2: A solar extreme ultraviolet flux model, Contribution 9, Earth and Planet. Atmos. Group, Space Sci. Lab., Univ. of Calif., Berkeley, 1990.
- Tobiska, W. K., Revised solar extreme ultraviolet flux model, *J. Atmos. Terr. Phys.*, 53, 1005-1018, 1991.
- Tobiska, W. K., and C. A. Barth, A solar EUV flux model, *J. Geophys. Res.*, 95, 8243-8251, 1990.
- Tobiska, W. K., S. Chakrabarti, G. Schmidtke, and H. Doll, Comparative solar EUV flux for the San Marco ASSI, *Adv. Space Res.*, 13, (1)255-259, 1993.
- Tousey, R., Solar spectroscopy in the far ultraviolet, *J. Opt. Soc. Am.*, 51, 384-395, 1961.
- Vernazza, J. E., E. H. Avrett, and R. Loeser, Structure of the solar chromosphere, III, Models of the EUV brightness components of the quiet sun, *Ap. J., Suppl. Ser.*, 45, 635-725, 1981.
- Vidal-Madjar, A., The solar spectrum at Lyman-alpha 1216 Å, in *The Solar Output and Its Variation*, edited by O. R. White, pp. 213-236, Colorado Associated University Press, Boulder, Colo., 1977.
- Wagner, W. J., Observations of 1-8 Å solar x-ray variability during solar cycle 21, *Adv. Space Res.*, 8, 67-76, 1988.
- Winningham, J. D., D. T. Decker, J. U. Kozyra, J. R. Jasperse, and A. F. Nagy, Energetic (> 60 eV) atmospheric photoelectrons, *J. Geophys. Res.*, 94, 15,335-15,348, 1989.
- White, O., The solar spectrum, in *The Solar Output and Its Variation*, edited by O. R. White, pp. 25-28, Colorado Associated University Press, Boulder, Colo., 1977.
- White, O. R., Ground-based surrogates for UV and EUV fluxes, in *Solar Radiative Output Variation*, edited by P. Foukal, pp. 88-112, Cambridge Research and Instrumentation, Cambridge, Mass., 1987.
- White, O. R., and W. C. Livingston, Solar luminosity variation. II. Behavior of Calcium H and K at solar minimum and the onset of cycle 21, *Ap. J.*, 226, 679-686, 1978.
- White, O. R., and W. C. Livingston, Solar luminosity variation, III, Calcium K variation from solar minimum to maximum in cycle 21, *Ap. J.*, 249, 798-816, 1981.
- Woods, T. N., and G. R. Rottman, Solar EUV irradiance derived from a sounding rocket experiment on November 10, 1988, *J. Geophys. Res.*, 95, 6227-6236, 1990.
- Zirin, H., Variability of solar ultraviolet emission, in *Solar Radiative Output Variation*, edited by P. Foukal, pp. 301-308, Cambridge Research and Instrumentation, Cambridge, Mass., 1987.

W. K. Tobiska, TELOS/JPL, MS 264-765, 4800 Oak Grove Dr., Pasadena, CA 91109.

(Received October 19 1992;
revised January 20, 1993;
accepted March 3, 1993.)